FEBS 26289

FEBS Letters 523 (2002) 247–251

First tau repeat domain binding to growing and taxol stabilized microtubules, and serine 262 residue phosphorylation

François Devred, Soazig Douillard, Claudette Briand, Vincent Peyrot*

UMR CNRS 6032, Faculté de Pharmacie, 27 Boulevard Jean Moulin, 13385 Marseille Cedex 5, France

Received 9 April 2002; revised 5 June 2002; accepted 10 June 2002

First published online 28 June 2002

Edited by Thomas L. James

Abstract **Tau phosphorylation plays a crucial role in microtubule stabilization and in Alzheimer's disease. To characterize the molecular mechanisms of tau binding on microtubules, we synthesized the peptide R1 (QTAPVPMPDLKNVKSKIGSTENLKHQPGGGKVQI), reproducing the first tau microtubule binding motif. We thermodynamically characterized the molecular mechanism of tubulin assembly with R1 in vitro, and measured, for the first time, the binding parameters of R1 on both growing and taxol-stabilized microtubules. In addition, we obtained similar binding parameters with R1 phosphorylated on Ser262. These data suggest that the consequences of Ser262 phosphorylation on tau binding to microtubules and on tubulin assembly are due to large intramolecular rearrangements of the tau protein.** **© 2002 Federation of European Biochemical Societies. Published by Elsevier Science B.V. All rights reserved.**

Key words: Tubulin; Tau; Microtubule; Peptide; Phosphorylation; Serine 262

1. Introduction

Microtubule functions are regulated by microtubule-associated proteins (MAPs) such as tau or Map2. Tau is the most studied because of its implication in Alzheimer's disease [1,2] as the main constituent of paired helical filaments (PHFs). The C-terminal domain of tau proteins bears three to four homologous 31/32 amino acid repeats (R1, R2, R3, R4) [1], which constitute the microtubule binding domains, some of which can bind to free tubulin [3] or to microtubule-incorporated tubulin [4,5] and promote tubulin assembly by themselves [6,7]. Repeat R1 binds more efficiently [8] and induces tubulin polymerization with a greater capacity [6]. Furthermore, this domain is believed to play a crucial role in tau processes, being the target of specific phosphorylations. Indeed, phosphorylation appears to be the most critical step in the biological and pathological processes implicating tau.

Many microtubule–MAP interaction studies have been carried out using taxol-stabilized microtubules and different constructs or peptides corresponding to the repeat domains of tau or Map2c [9]. Of all the described tau phosphorylation sites [10], Ser262 is the only site in the first repeat domain R1. Some discrepancy exists in the literature concerning the role of this particular phosphorylation site. One study showed that phosphorylation of Ser262 was not sufficient to eliminate the binding of tau to microtubules [11], whereas a second one showed that Ser262 phosphorylation abolished tau binding to microtubules regardless of the phosphorylation state of flanking domains [12]. More recently, the involvement of Ser262 phosphorylation for inhibition of tau binding was stressed again [13].

To clearly answer the question of R1 and Ser262 involvement in tau binding to microtubules we synthesized peptide R1, corresponding to the whole first tau repeat and its phosphorylated counterpart on Ser262, R1p. We first characterized the influence of R1 on the molecular mechanism of tubulin assembly, determining the thermodynamic parameters of the process and the Mg^{2+} intake with and without R1. From this point, we quantitatively studied R1 interaction with microtubules in vitro. We measured the binding parameters of R1 on growing microtubules, by extrapolation of the polymerization curves, as well as on taxol-stabilized microtubules, by co-sedimentation assay. Last, to investigate the direct consequence of phosphorylation on R1, we carried out the same quantitative binding study with R1p. The data support the notion of an intramolecular conformational change upon tau binding to microtubules and led us to speculate on the mechanisms by which phosphorylation of tau, by detaching it from the microtubules, might lead to formation of PHFs in Alzheimer's disease.

2. Materials and methods

2.1. Tubulin purification

Tubulin was purified from pig brains as previously described in [14]. Protein concentrations were determined spectrophotometrically with an extinction coefficient of $\varepsilon_{275\ nm} = 1.09\ l\ g^{-1}\ cm^{-1}$ in 6 M guanidine hydrochloride [14].

2.2. Peptide synthesis

R1 and R1p peptides were synthesized in Fmoc solid phase synthesis [15] with HMP (4-hydroxymethyl–phenoxymethyl copolystyrene–1% divinylbenzene) preloaded resin (0.5–0.65 mmol) (Perkin-Elmer, Applied Biosystems Inc.). Peptides were deprotected and released from the resin by trifluoroacetic acid treatment. Peptide R1 (QTAPVPMPDLKNVKSKIGSTENLKHQPGGGKVQI) corresponds to amino acids 244–277 of the human tau [1]. R1p is the same sequence with a phosphorylated residue on Ser262. Peptide purity was assessed by amino acid composition and high-performance liquid chromatography (HPLC).

2.3. Tubulin assembly and co-sedimentation assay

Tubulin assembly was performed as described previously [16]. In PEMG buffer (20 mM sodium phosphate buffer, 1 mM EGTA (ethylene glycol-bis(2-aminoethyl-ether)-*N*,*N*,*N*′,*N*′-tetraacetic acid), 10 mM

*Corresponding author. Fax: (33)-491835505.
E-mail address: vincent.peyrot@pharmacie.univ-mrs.fr (V. Peyrot).

Abbreviations: Cr, critical concentration; MAP, microtubule-associated protein; PHF, paired helical filament

PII: S0014-5793(02)02999-X

$MgCl_2$, 3.4 M glycerol, 0.1 mM GTP (guanosine triphosphate) pH 6.5) co-sedimentation assay was performed as described [7] with one modification. We used a cushion of glycerol [8] during the centrifugation step to eliminate non-specific binding. The supernatants were then analyzed by HPLC (Pharmacia ÄKTA Purifier 900) using a reverse phase column (Source 15RPC ST4.6/100) with a linear gradient of 0–80% acetonitrile in 0.1% trifluoroacetic acid. Using a calibration curve, we determined peptide concentration by absorbance at 210 nm. Experiments were done in triplicate.

2.4. Apparent thermodynamic parameters of R1-induced microtubule assembly

Thermodynamic parameters can be obtained from the Van 't Hoff plot of tubulin polymerization as described by Lee et al. [17] with the equation

$$\ln K_{app} = a + b\left(\frac{1}{T}\right) + c(\ln T) \quad (1)$$

where K_{app} is the apparent equilibrium constant for the growth reaction ($K_{app} = Cr^{-1}$, with Cr the critical concentration). The values of free energy (ΔG^0), enthalpy (ΔH^0), entropy (ΔS^0) and heat capacity (ΔC_p) are given by the following equations:

$$\Delta G^0_{app} = -RT\ln K_{app}$$

$$\Delta H^0_{app} = R(cT - b)$$

$$\Delta S^0_{app} = \frac{(\Delta H^0_{app} - \Delta G^0_{app})}{T}$$

and

$$\Delta C_p = R \times c$$

2.5. Determination of the binding parameters of the peptide on growing microtubules

Ligand binding parameters were determined using Timasheff's model [18]. The model can be expressed through a set of equations leading to the final one:

$$K_{gapp} = K_g \times (1 + K_b \times P)^{1/n} \quad (2)$$

one molecule of P being added for each n-tubulin dimer incorporated into microtubules. K_{gapp} is the experimentally determined growth constant, which is the inverse of Cr in the presence of P, K_g is the inverse of Cr without P, and K_b the binding constant of P to the microtubule. Based on previous studies [19], we expected a low binding constant and made the approximation (proven correct) that free P is very similar to total P. All the fittings were done using a graphics-fitting program (Sigmaplot 4.0, Jandel Scientific).

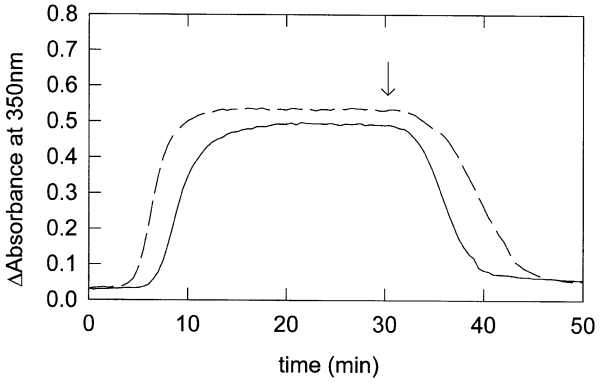

Fig. 1. Representative curves of polymerization followed by turbidity. The tubulin assembly curve is given as a solid line, whereas tubulin polymerization with 400 μM R1 is given as a dashed line. Tubulin concentration is 13 μM. Polymerization is started by heating the samples to 37°C. At the time indicated by the arrow, the samples were cooled to 10°C.

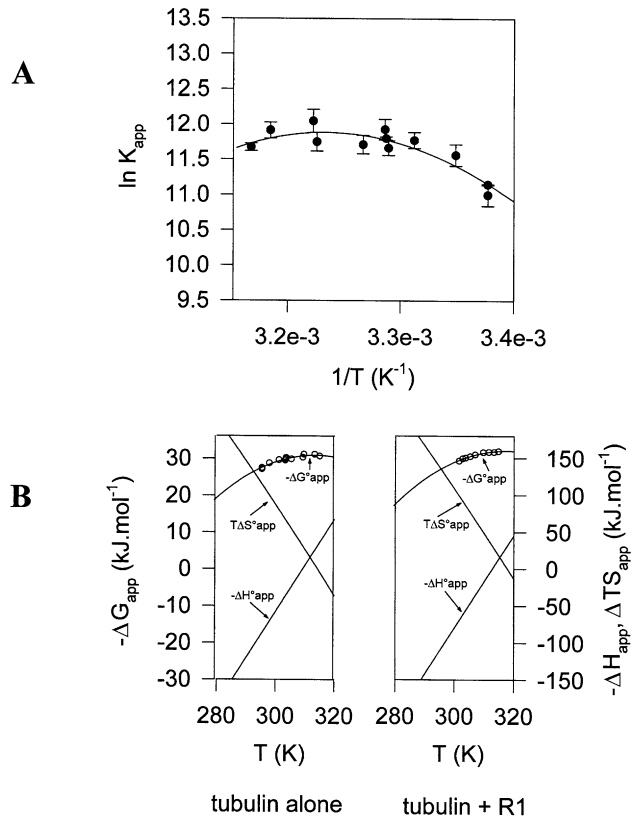

Fig. 2. Thermodynamics of tubulin assembly. A: Van 't Hoff plot of the microtubule growth reaction in PEMG buffer. The Crs used to determine the K_{app} were measured at temperatures ranging from 23 to 43°C. The solid line is the theoretical curve obtained by fitting a, b and c (see Section 2). B: Enthalpy and entropy contributions to the apparent standard free energy change of elongation of tubulin in PEMG buffer of tubulin alone (left panel), and of tubulin with 345 μM R1 (right panel). The dots on the ΔG^0_{app} curve represent the experimental points from the Van 't Hoff plot. All the other points (solid line) were calculated and extrapolated (see Section 2). Each point represents the average of several experiments with different tubulin preparations.

3. Results

3.1. Thermodynamic parameters of tubulin assembly in the presence of peptide R1

Tubulin assembly is greater in the presence of peptide R1, but the overall shape of the polymerization is the same as that followed by turbidimetry (Fig. 1). We verified by electronic microscopy (data not shown) that the polymers were normal microtubules. We determined that the minimum tubulin Cr for polymerization ($Cr = 4.0 \pm 0.7$ μM) is reached with 345 μM R1 (at 37°C). It corresponds to about a two-fold decrease, compared to polymerization without peptide ($Cr = 7.0 \pm 0.5$ μM) (data not shown). The effects of temperature on tubulin self-association were examined in PEMG buffer for tubulin alone and in the presence of the peptide (345 μM). As described for tubulin alone [17], a pronounced curvature is observed in the Van 't Hoff plot of tubulin assembly with peptide (Fig. 2A). From Eq. 1 (see Section 2) we deduced the apparent change in heat capacity $\Delta C_p = -1495 \pm 386$ cal/(mol deg) of tubulin dimer added as well as ΔG^0_{app}, ΔH^0_{app}, ΔS^0_{app} (see Fig. 2B) of this reaction. With peptide R1 we obtained the same value of ΔC_p (-1493 ± 450

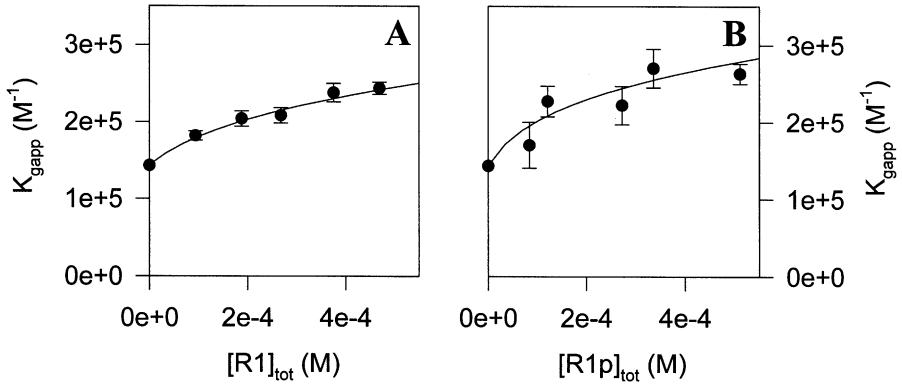

Fig. 3. Extrapolation of the polymerization curves leading to the binding parameters of tubulin assembly: (A) tubulin in the presence of various concentrations of R1 and (B) in the presence of various concentrations of R1p. The solid line is the theoretical curve obtained by fitting n and K_b (see Section 2). The points represent averages of multiple experiments.

cal/(mol deg)) and very similar thermodynamic profiles (Fig. 2B), indicating that the overall thermodynamic parameters are not significantly affected. Last, to determine the Mg^{2+} intake during the polymerization process, Mg^{2+} being an essential cofactor in tubulin polymerization [20,21], we calculated the Cr for different concentrations of Mg^{2+}, in the presence of a fixed concentration of R1 (345 μM). Using the Wyman plot analysis described by Lee et al. [17], we found a slope of 1.1 ± 0.2 (data not shown), which indicates a difference in preferential interaction of one additional Mg^{2+} per tubulin molecule incorporated into microtubules, similar to the case for tubulin alone.

All these results indicate that R1 favors polymerization without disturbing the polymerization process, in contrast to other stabilizing agents such as taxol, for which both polymerization thermodynamic parameters and Mg^{2+} ions incorporated are affected [22].

3.2. *Determination of the binding parameters of R1 and R1p on growing microtubules by polymerization curve extrapolation*

Using a set of different polymerization curves for various concentrations of R1 we plotted K_{gapp} as a function of R1 concentration (Fig. 3A). Using Eq. 2 we found the affinity binding constant of the peptide for microtubules $K_b = (1.56 \pm 0.67) \times 10^4$ M^{-1} and the number of dimers incorpo-

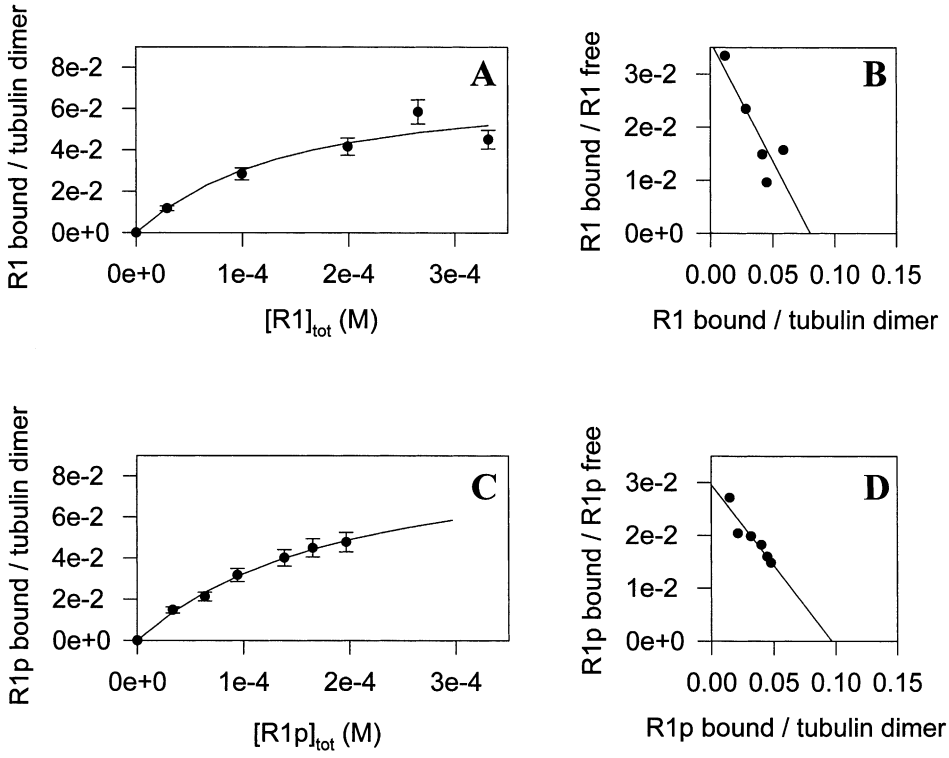

Fig. 4. Microtubule binding activity of R1 and R1p. (A) and (C) are the saturation curves of R1 and R1p, respectively. (B) and (D) are the corresponding Scatchard plots. The tubulin dimer concentration incorporated in microtubules was calculated by subtracting the amount of tubulin that did not polymerize (Cr) from the total tubulin concentration used in the assay. Each point represents the average of several binding experiments. In the Scatchard plots, axes are molar ratios.

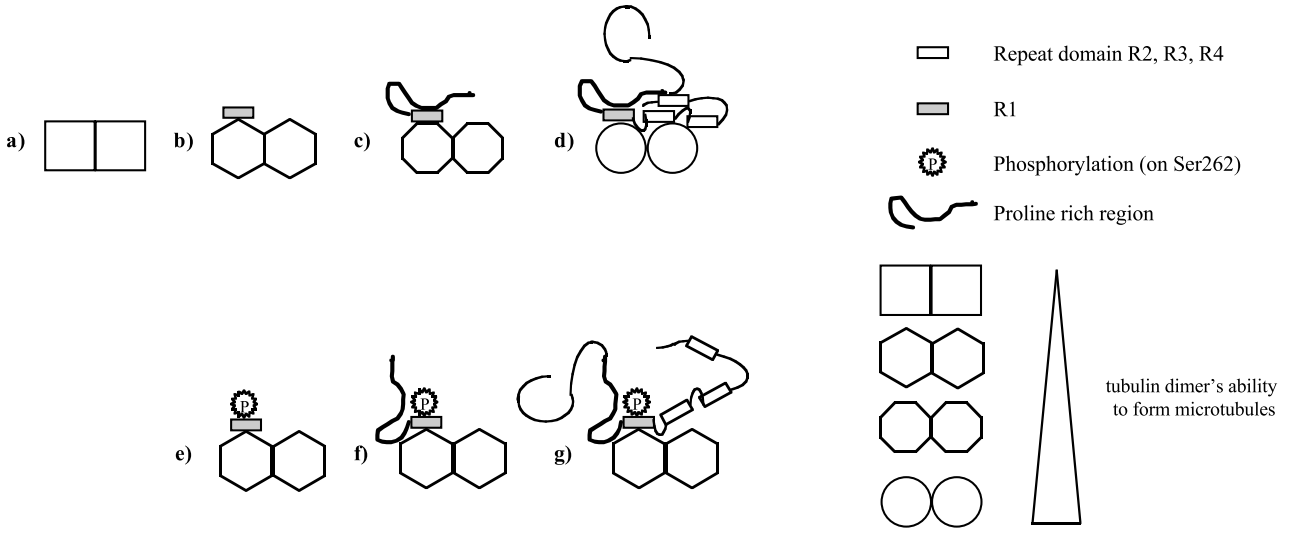

Fig. 5. Schematic representation of conformational change and binding interaction of tau to microtubule: (a) is a regular tubulin dimer; (b) represents the probable conformational change of tubulin due to peptide R1 binding; (c) shows a larger conformational change, correlated to the 10-fold increase in assembly in the presence of the proline-rich region observed by Goode et al. [32]; (d) shows a possible model of tau binding to tubulin in which tau adopts a more complex ordered structure involving intramolecular interactions between the repeats and the proline-rich region. Tau binding in turn guides the tubulin dimer into a stable, folded pro-microtubule conformation; (e) shows no difference compared to (b) as demonstrated in this paper; (f) and (g) hypothesize the lack of pro-microtubule effect by the flanking domains when the protein is phosphorylated on Ser262. Ser262 phosphorylation prevents the conformational change necessary for maximum assembly efficiency. The effect observed is only due to the binding of R1 (case (b)). The isoforms of tubulin (α and β) were voluntarily omitted to insist on the fact that the peptide probably binds both of them.

rated in microtubules per mol of peptide bound $n = 3.95 \pm 0.78$. With R1p (Fig. 3B) we obtained $K_b = (3.28 \pm 2.95) \times 10^4$ M^{-1} and $n = 4.49 \pm 2.25$. In both cases binding constants and stoichiometry are similar; one peptide for about four dimers was incorporated into a microtubule.

3.3. Direct measurement of the binding parameters of R1 and R1p on taxol-stabilized microtubules

We also compared by a quantitative co-sedimentation assay the microtubule affinity of both peptides by directly measuring their binding constants on preformed taxol-stabilized microtubules. Fig. 4A,C shows the saturation curves of R1 and R1p in the range of concentrations used (0–200 μM for R1 and 0–350 μM for R1p). Scatchard plots (Fig. 4B,D) correspond to a binding constant of $K_b = (0.64 \pm 0.22) \times 10^4$ M^{-1} for R1 and $K_b = (0.51 \pm 0.10) \times 10^4$ M^{-1} for R1p. These values are similar. We found stoichiometries of $n' = 0.08 \pm 0.04$ and $n' = 0.10 \pm 0.02$ per dimer of tubulin for R1 and R1p, respectively, which corresponds to a stoichiometry of about one tau peptide for every 10 dimers.

4. Discussion

Up to now, experiments had been conducted to test the influence of phosphorylation on other repeat domains [23], but no direct measurement had been made between the phosphorylated R1 domain and the entire tubulin in microtubules, in which conformation change might occur. In our study on Ser262 of R1 repeat, phosphorylation modifies neither the apparent binding constant nor the stoichiometry of R1 domain binding on microtubules. These results clearly show that phosphorylation on Ser262 of R1 repeat is not sufficient to induce its detachment or to diminish tubulin assembly. Furthermore, the relatively small difference in binding constant between the two protocols for R1 or R1p is in favor of a binding site easily accessible on the lattice of the microtubule, since the state of the microtubule, growing or stabilized, makes no difference. In both cases we find a constant in good agreement with the one determined in different buffer conditions (PIPES, EGTA, Mg^{2+} 1 mM) by Aizawa et al. ($K_b = 5550$ M^{-1}) for non-phosphorylated peptide [7]. This is a rather low apparent binding constant, 5000–10 000 M^{-1}, about 1000 times lower than tau itself. Considering that the summation of three to four repeat domains [8,24,25] is not sufficient to explain such a large binding constant, and that R1 has the strongest effect on microtubules [6,8], R1 is probably involved in the first steps of the binding, but there must be some conformational change in tau involving other domains of the protein, which enhances its binding on microtubules.

The differences we found in the stoichiometry, 0.1–0.25 peptide per tubulin dimer against 1.3 peptide per tubulin dimer found by Aizawa et al. [7], may be explained by the size of the peptide itself, 14 amino acids longer, but most of all by the use of a glycerol cushion in our co-sedimentation assay, which probably gets rid of non-specific binding [8]. Nevertheless, it is interesting to note that these surprisingly low stoichiometry values, especially considering that tau has been reported to bind both on α and β C-terminal parts of tubulin [26], are close to the one found for the entire tau protein [27] or other MAPs [28]. This would tend to rule out substoichiometry as an argument for tau binding longitudinally along the protofilament versus a bridging of the microtubules. It merely shows that steric hindrance is not responsible for the low stoichiometry of the tau protein. Nevertheless, this substoichiometric binding is sufficient to explain its stabilizing effect on the microtubule [29].

Phosphorylation of Ser262 clearly induces tau detachment of the microtubule with a decrease in binding stoichiometry and a destabilizing effect [12,30]. In contrast, this phosphory-

lation on R1 does not. The structure of tau, when bound at the microtubule surface, differs from the structure of the peptide itself. This result is again in favor of an intramolecular conformational modification implicating other domains of tau that would influence R1 binding efficiency.

The flanking regions, which have been shown to play an important part since their phosphorylation detaches the tau protein or diminishes its affinity [13,31], are good candidates for these intramolecular interactions. Among these, the proline-rich domain causes a 10-fold increase in the efficiency of peptide-induced microtubule assembly when joined to the R1+R1R2 inter-repeat sequence [32]. Our data are also compatible with an interaction between the proline-rich domain and repeat regions of tau. This model, summarized in Fig. 5, would explain why phosphorylation has a dual effect depending on the construct. With R1, no difference is observed upon phosphorylation, whereas on bigger constructs (with flanking domains) and on the entire tau, phosphorylation on Ser262 prevents the conformational change necessary for better tubulin assembly induction and favors detachment of tau from the microtubule. Further phosphorylation on additional specific sites then leads to PHF formation [33]. Ser262 phosphorylation is thus a key step both in the physiological regulation of microtubule assembly and in the pathological induction of PHFs in Alzheimer's disease, but in both cases it implicates the flanking domains of tau.

Acknowledgements: We thank Dr. Pascale Barbier for scientific and technical help, Dr. Jean Michel Verdier (EPHE, Montpellier) for helpful discussions and Dr. Erwann Loret (CNRS–IBSM, Marseille) for peptide synthesis.

References

[1] Goedert, M., Wischik, C.M., Crowther, R.A., Walker, J.E. and Klug, A. (1988) Proc. Natl. Acad. Sci. USA 85, 4051–4055.
[2] Jakes, R., Novak, M., Davison, M. and Wischik, C.M. (1991) EMBO J. 10, 2725–2729.
[3] Maccioni, R.B., Vera, J.C., Dominguez, J. and Avila, J. (1989) Arch. Biochem. Biophys. 275, 568–579.
[4] Himmler, A., Drechsel, D., Kirschner, M.W. and Martin Jr., D.W. (1989) Mol. Cell Biol. 9, 1381–1388.
[5] Lee, G., Neve, R.L. and Kosik, K.S. (1989) Neuron 2, 1615–1624.
[6] Ennulat, D.J., Liem, R.K., Hashim, G.A. and Shelanski, M.L. (1989) J. Biol. Chem. 264, 5327–5330.
[7] Aizawa, H., Kawasaki, H., Murofushi, H., Kotani, S., Suzuki, K. and Sakai, H. (1989) J. Biol. Chem. 264, 5885–5890.
[8] Butner, K.A. and Kirschner, M.W. (1991) J. Cell Biol. 115, 717–730.
[9] Coffey, R.L. and Purich, D. (1995) J. Biol. Chem. 270, 1035–1040.
[10] Buee, L., Bussiere, T., Buee-Scherrer, V., Delacourte, A. and Hof, P.R. (2000) Brain Res. Rev. 33, 95–130.
[11] Seubert, P., Mawal-Dewan, M., Barbour, R., Jakes, R., Goedert, M., Johnson, G.V., Litersky, J.M., Schenk, D., Lieberburg, I., Trojanowski, J.Q. and Lee, V.M.Y. (1995) J. Biol. Chem. 270, 18917–18922.
[12] Drewes, G., Trinczek, B., Illenberger, S., Biernat, J., Schmitt-Ulms, G., Meyer, H.E., Mandelkow, E.M. and Mandelkow, E. (1995) J. Biol. Chem. 270, 7679–7688.
[13] Sengupta, A., Kabat, J., Novak, M., Wu, Q., Grundke-Iqbal, I. and Iqbal, K. (1998) Arch. Biochem. Biophys. 357, 299–309.
[14] Barbier, P., Peyrot, V., Leynadier, D. and Andreu, J.M. (1998) Biochemistry 37, 758–768.
[15] Merrifield, G. and Barany, R.B. (1980) The Peptide: Analysis, Synthesis, Biology, Academic Press, New York.
[16] Barbier, P., Gregoire, C., Devred, F., Sarrazin, M. and Peyrot, V. (2001) Biochemistry 40, 13510–13519.
[17] Lee, J.C. and Timasheff, S.N. (1977) Biochemistry 16, 1754–1764.
[18] Timasheff, S.N. (1978) in: Thermodynamic examination of the self-association of brain tubulin to microtubules and other structures (Catsimpoolas, N., Ed.), pp. 219–273, Elsevier/North-Holland.
[19] Joly, J.C. and Purich, D.L. (1990) Biochemistry 29, 8916–8920.
[20] Menendez, M., Rivas, G., Diaz, J.F. and Andreu, J.M. (1998) J. Biol. Chem. 273, 167–176.
[21] Bhattacharya, A., Bhattacharyya, B. and Roy, S. (1994) J. Biol. Chem. 269, 28655–28661.
[22] Diaz, J.F., Menendez, M. and Andreu, J.M. (1993) Biochemistry 32, 10067–10077.
[23] Hoffmann, R., Dawson, N.F., Wade, J.D. and Otvös Jr., L. (1997) J. Pept. Res. 50, 132–142.
[24] Goode, B.L. and Feinstein, S.C. (1994) J. Cell Biol. 124, 769–782.
[25] Gustke, N., Trinczek, B., Biernat, J., Mandelkow, E.M. and Mandelkow, E. (1994) Biochemistry 33, 9511–9522.
[26] Chau, M.F., Radeke, M.J., de Ines, C., Barasoain, I., Kohlstaedt, L.A. and Feinstein, S.C. (1998) Biochemistry 37, 17692–17703.
[27] Hirokawa, N., Shiomura, Y. and Okabe, S. (1988) J. Cell Biol. 107, 1449–1459.
[28] Jensen, C.G. and Smaill, B.H. (1986) J. Cell Biol. 103, 559–569.
[29] Panda, D., Goode, B.L., Feinstein, S.C. and Wilson, L. (1995) Biochemistry 34, 11117–11127.
[30] Biernat, J., Gustke, N., Drewes, G., Mandelkow, E.M. and Mandelkow, E. (1993) Neuron 11, 153–163.
[31] Gustke, N., Steiner, B., Mandelkow, E.M., Biernat, J., Meyer, H.E., Goedert, M. and Mandelkow, E. (1992) FEBS Lett. 307, 199–205.
[32] Goode, B.L., Denis, P.E., Panda, D., Radeke, M.J., Miller, H.P., Wilson, L. and Feinstein, S.C. (1997) Mol. Biol. Cell 8, 353–365.
[33] Morishima-Kawasaki, M., Hasegawa, M., Takio, K., Suzuki, M., Yoshida, H., Watanabe, A., Titani, K. and Ihara, Y. (1995) Neurobiol. Aging 16, 365–380.